CHINESE JOURNAL OF GEOPHYSICS Vol.52, No.6, 2009, pp: 1237∼1250

PRESENT-DAY GEOTHERMAL REGIME IN TARIM BASIN, NORTHWEST CHINA

FENG Chang-Ge[1], LIU Shao-Wen[2*], WANG Liang-Shu[1], LI Cheng[1]

1 *School of Earth Science and Engineering, Nanjing University, Nanjing* 210093*, China*

2 *Key Laboratory of Island and Coast Exploitation, Ministry of Education, School of Geographic and Oceanographic Sciences, Nanjing University, Nanjing* 210093*, China*

Abstract Geothermal gradient and surface heat flow are key parameters that describe the thermal regime of sedimentary basin, and are so vital for understanding the tectono-thermal evolution and associated hydrocarbon potential assessment of oil and gas bearing basin. Here we presented the distribution pattern of the updated present-day geothermal gradient and determined 38 surface heat flow values in the Tarim basin, the biggest sedimentary basins in China, on the basis of formation temperature data from approximately 470 wells and 941 measured thermal conductivities of rocks within this basin. Our results showed that the present-day geothermal gradient of Tarim basin varied between 17∼32 °C/km and with a mean of 22.6±3.0 °C/km, and the surface heat flow ranged from 26.2 to 65.4 mW/m^2 with a mean of 43.0±8.5 mW/m^2, suggesting its thermal regime as a cold basin of low temperature and heat flow, compared with other large-middle scale sedimentary basins in China. Accordingly, this low thermal regime also makes Tarim basin to share the similar thermal regime of other typical craton basins in the world. It is obvious that the geothermal gradient and surface heat flow in uplift areas are usually larger than those in the depressions, indicating the influence of configuration of basement on geothermal field pattern. We also found that the discovered oil and gas fields in Tarim are usually with relatively large geothermal gradient, the cause for this coincidence is not clear but the upward movement and accumulation of hot fluid below is speculated to account for this positive geothermal anomaly. Finally, we summarized the factors that influence the geothermal distribution of basin as deep structure, tectonic evolution and basement configuration of basin, thermal physical properties of rocks and hydrocarbon accumulation as well.

Key words Geothermal gradient, Thermal conductivity, Terrestrial heat flow, Geothermal regime, Tarim basin

1 INTRODUCTION

Located in northwest China, the Tarim basin is surrounded by the ranges of the Tianshan, Kunlun and Altyn Tagh mountains, and is also the biggest oil and gas bearing intermontane basin in China (Fig. 1). Considering its abundance in hydrocarbon potential, this basin is now and will be the target of oil and gas exploration in China during next decade for implementation of the national strategy of developing the west China and transferring natural gas from west to east China project. Previous studies have shown that the Tarim basin is one superimposed basin that is composed of the Paleozoic craton basin as the nucleus and encircled by young Meso-Cenozoic foreland basin in the margin, along with the continental crustal basement and episodic uplift and erosion histories during geological evolution[1]. The nature of present-day thermal regime of basin is the combined results of deep lithospheric thermodynamic process and tectonic evolution of basin as well, holding important role in oil and gas generation. Being the last episode of thermal evolution of the basin, the present-day geothermal regime not only provides thermal parameters for basin modeling and associated hydrocarbon assessment, but also constraints on the analysis of tectono-thermal evolution and basin formation. Investigating the present-day geothermal regime of sedimentary basin is a long lasting topic in the academic and industry communities.

Since 1980s, considerable advancements on the geothermal characteristics of the Tarim basin have been made and indicated the general features of geothermal regime as low heat flow and cold basin[2∼8]. For example, Wei[2] firstly retrieved six heat flow values from the Kuqa-Luntai areas in the north Tarim basin, ranging

*Corresponding author: shaowliu@nju.edu.cn

43∼44 mW/m^2, and Zhang et al.[3] discussed the relationship between thermal regime and oil & gas distribution on the basis of formation temperature data from 37 boreholes. Wang et al.[4] and Wang et al.[5] then reported some new heat flow data of this basin and presented its general distribution pattern, their results show that the surface heat flow of this basin varies from 40 to 50 mW/m^2, and is featured by low values occurred in the edge area and high in the basin interior. Although these studies mentioned above put emphasis on the whole basin pattern, much more related works were only devoted to the geothermal regime of local regions of this basin. For example, Xie[6] studied the geothermal characteristics in the northern Tarim basin, and inferred that the present-day geothermal gradient there is about 20°C/km; Wang et al.[7,8] made a case study of the Kuqa foreland basin in northern Tarim, to decipher the pattern of present-day geothermal gradient and heat flow. Based on compilation of previous data and some new measured values in this basin, Qiu[9] firstly reported the data of formation thermal conductivity and heat generation in the Tarim basin systematically, and discussed the relationship of these data with burial depth and other physical properties.

Although previous studies are relevant to the geothermal regime of the Tarim basin to different extent, these results have been obtained two decades ago, especially, the data used in analysis are really sparse. Actually most of previous investigations only cover the Kuqa and Luntai area in the north of Tarim basin, and the thermal regime of the left regions in this big basin remains poorly known. With the increasing enlargement of oil and gas exploration in this basin, many new formation temperature data and physical properties are available. A revisiting geothermal regime of this basin is essential for hydrocarbon assessment concerned. In this study, all the new temperature data are combined with previous data to reveal the present-day geothermal regime of the Tarim basin, and the factors that influence subsurface geothermal pattern are discussed. The result shown here is representative of the updated understanding of geothermal regime of this basin. Of particularly interest, it is found that the discovered oil and gas fields in this basin coincide well with the regions where the geothermal gradient is relatively high (positive geothermal anomaly), this finding is of significance for oil and gas exploration as one possible geothermal tool.

2 TEMPERATURE DATA CLASSIFICATION AND ANALYSIS

Formation temperature data that are used in studying thermal regime of sedimentary basin are measured in borehole with different purposes and requirements. The common temperature data can be classified into different types as the continuous temperature logging data, temperature derived from formation testing (equilibrium temperature and fluid temperature), borehole temperature (BHT), and etc. Among these data, the continuous temperature logging data and formation testing temperature are considered to be more reliable, due to enough shut in time for recovery, constituting the main data sources for study of temperature field of basin. Nevertheless, other temperature data that lacks of enough equilibrium time, such as the BHT, but can also be used for geothermal analysis after correction. Unfortunately, continuous temperature logging is usually rare in oil exploration, so most formation testing temperature and corrected BHT data are used here.

2.1 Continuous Temperature Logging Data

The continuous temperature logging is conducted in the borehole that has been ceased and preserved for several or ten days, even more than half a year, and the temperature is recorded in 10 or 20 m intervals continuously when the thermometer going down. The temperature of this type should have returned to its equilibrium state, due to long duration of cessation, representative of true formation temperature. 44 temperature loggings are available in the Tarim basin, and 27 of them, with longer shut-in time, are selected here for thermal regime analysis (as shown in Fig. 1 and Fig. 2a). The intersection of temperature profile with horizontal axis approximates to the annual average surface temperature in Xinjiang area, also indicating the borehole was under thermal equilibrium state at that time. As shown in the temperature profile in Fig. 2a, the temperature data show a linear general trend with depth, which is the typical feature of conductive heat transferring process. However, variation is also observed in some temperature profiles, maybe influenced by underground water

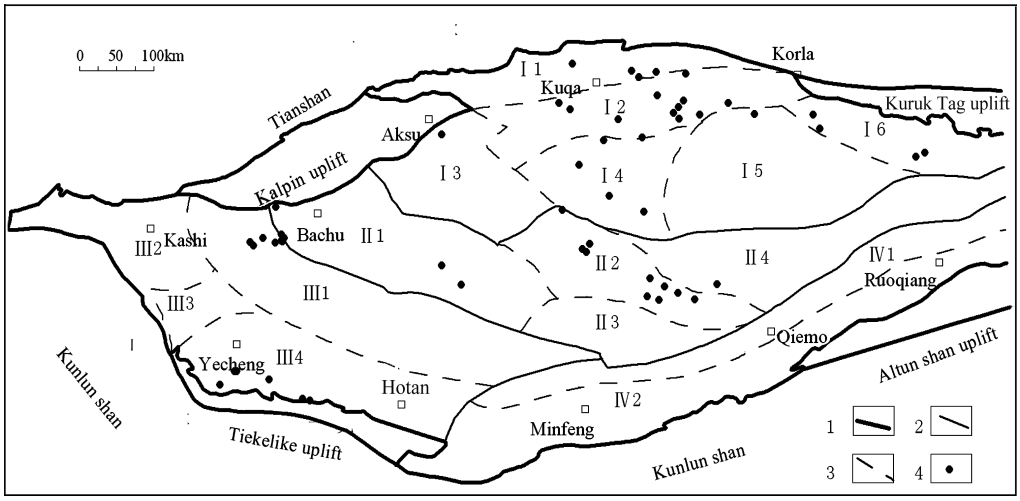

Fig. 1 Sketch showing the tectonic subdivision and temperature logging boreholes of Tarim basin

1 Basin boundary; 2 Primary boundary; 3 Secondary boundary; 4 Systematically temperature logging borehole. I. Northeast depression: I1. Kuqa depression; I2. Shaya uplift; I3. Awat faulted depression; I4. Shuntuoguole uplift; I5. Manjiaer depression; I6. Kongquehe slope. II. Central uplift: II1. Bachu uplift; II2. Katake uplift; II3. Tanggubasi depression; II4. Guchengxu uplift. III. Southwest depression: III1. Maigaiti slope; III2. Kashi depression; III3. Shache uplift; III4. Yecheng depression. IV. Southeast faulted uplift: IV1. Northminfeng-Luobuzhuang faulted uplift; IV2. Yutian-Ruoqiang depression.

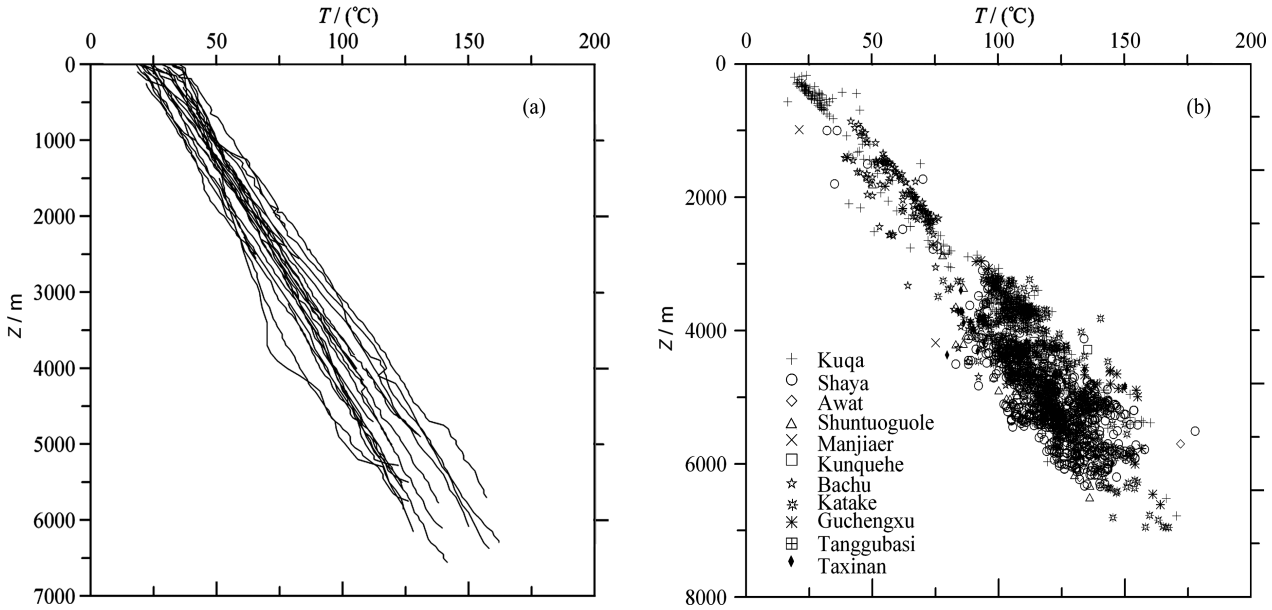

Fig. 2 Variations of temperature in borehole with depth in Tarim basin

(a) Continuous temperature logging data; (b) Formation oil testing temperature data.

disturbance, so these intervals should be avoided when calculating heat flow. It should be mentioned that, these 27 boreholes are really sparsely distributed geographically, and mainly concentrate in the Shaya area of the northern Tarim basin. To overcome this uneven coverage for this whole basin scale study, many formation testing temperature data are adopted here as supplementation.

2.2 Formation Testing Temperature Data

Formation testing temperature data here refers to the data that were measured in borehole during reservoir testing on formation fluid with several days of shut in time after cessation. Occasionally, to test the different

oil bearing intervals in the same borehole, multiple measurements with different depths are available. Considering the cessation time is acceptable, the data of this type is also considered as representative of formation temperature. In this study, more than 2000 data from 424 boreholes are collected, and some obviously poor quality data were removed to avoid distorting temperature trends. As in Fig. 2b, the temperature increases linearly with increasing depth, indicating the temperature is in equilibrium with the formation temperature. The dataset that are retrieved from the same borehole and show linear trend with depth in different regions of the Tarim basin, are selected to calculate the geothermal gradient.

2.3 Geothermal Gradient

The geothermal gradient of the borehole where the continuous temperature logging data is available is determined by least square fitting method. If obvious subdivision is observed in the temperature profile, then each interval is fitted separately, and the mean gradient of different parts is considered as the gradient of this borehole. Similarly, the least square method is also applied for the borehole that has much formation testing temperature data.

While for the wells that have only one or two formation testing temperature data, the gradient is calculated by the following formula, given the known depth (Z_0) and temperature (T_0) of the constant temperature zone. In this study, Z_0 and T_0 are adopted as 20 m and 12°C, respectively[7]. The geothermal gradient (G) at the depth of Z is:

$$G = \frac{T - T_0}{Z - Z_0}.$$

The arithmetic average of gradient at different depths is considered here as the gradient of the borehole. The distribution pattern of present-day geothermal gradient of the Tarim basin is then available on the basis of these gradient data.

Our results show that the present-day geothermal gradient of the Tarim basin ranges from 17 to 32 °C/km, with a mean of 22.6±3.0 °C/km. As in Table 1, the average gradient of different tectonic sub-divisions of this basin is between 18 and 26 °C/km. Of particularly interest, the gradient is relatively high in the uplift areas with a value of 20∼26 °C/km, but is low in the depression areas as 18∼22 °C/km, suggesting the control of burial depth and basement topography on the distribution of present-day geothermal gradient.

The distribution pattern of present-day geothermal gradient of the Tarim basin is illustrated in Fig. 3. However, keep in mind that two sub-areas in the Tarim basin, the Kalpin uplift area in the northwest and Dongnan uplift area in the southeast, are not covered due to lack of data. It is found that the lowest geothermal gradient occurs in the Manjiaer and Yecheng depressions where the depth of base is also the largest, but the

Table 1 Present-day geothermal gradient of different structural subdivisions in Tarim basin

Primary tectonic units	Secondary tectonic units	Average gradient (°C/km)
Southwest depression	Kashi depression	19.8
	Yecheng depression	18.5
	Maigaiti slope area	22.9
Central uplift	Bachu uplift	23.6
	Katake uplift	23.4
	Tanggubasi depression	20.0
	Guchengxu uplift	24.3
Northeast depression	Kuqa depression	26.0
	Shaya uplift	21.5
	Awat uplift	22.4
	Shuntuoguole uplift	19.7
	Manjiaer depression	20.9
	Kongquehe slope	23.1

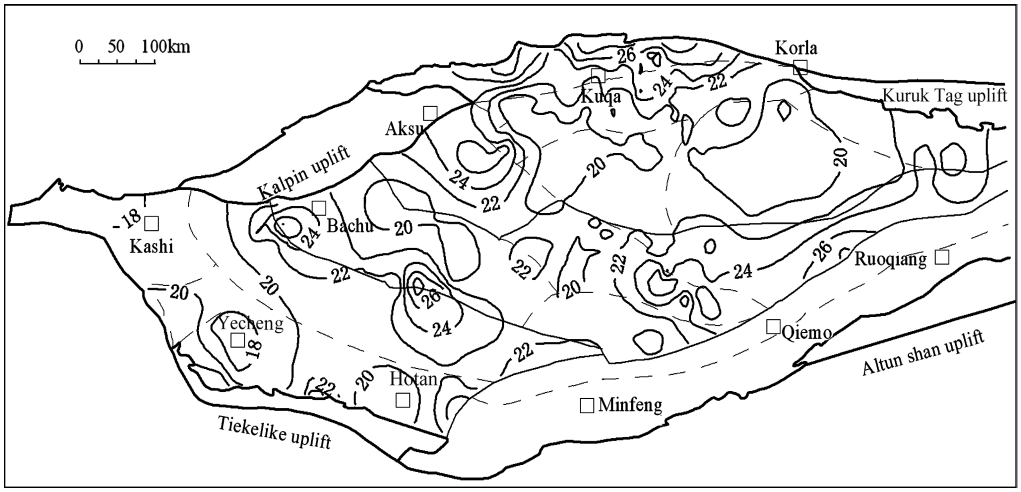

Fig. 3 Distribution pattern of present-day geothermal gradient in the interior of the Tarim basin

Kuqa depression in northern Tarim basin is characterized by relatively high geothermal gradient of 26 °C/km. Nevertheless, the gradient in the northern Bachu uplift area where the basement is relatively shallow, is somewhat low as 20 °C/km. These anomalous gradients mentioned will be further discussed in later section. It is obvious that the gradient decreases southwards gradually from 26∼28 °C/km in the linear anticline belt of the Kuqa depression near the Tianshan Mountain, to 20∼22 °C/km in the southern Shaya uplift. The mechanism of this southward decline in gradient is not clear, and we speculated that it is the result of weakening in Cenozoic coupled deformation between the Tianshan range with the Tarim basin from the margin to the interior of the basin.

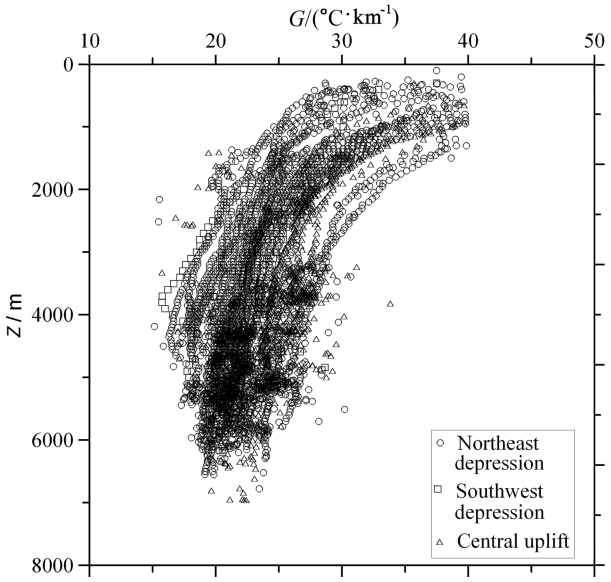

Fig. 4 Relationship between present-day geothermal gradient and depth of Tarim basin

Besides the obvious lateral variation of present-day geothermal gradient in the Tarim basin presented above, the gradient is also found to change with depth vertically. As in Fig. 4, the gradient decreased from 30 °C/km in shallow portion (the depth is less than 1000 m) to approximately 20 °C/km in the deep subsurface (near to 6000 m in depth), indicating the change in lithology and the influence of variation in thermal physical properties of rocks on geothermal gradient. With the increase of depth, the consolidation and compaction of the formation enhances gradually, resulting in the decline of porosity of rocks, consequently, this process will increase the thermal conductivity of rocks. Giving constant heat flow in borehole, elevation in thermal conductivity undoubtedly results in the decline in gradient. On the other side, decline in gradient with depth maybe is related to rapid subsidence of the basin. It is shown that the subsidence rate of Kuqa formation in the Yakela high of the Shaya uplift area is as large as 540 ∼880 m/Ma and 100 m/Ma for the Kangcun formation[6]. The sediment is usually low in thermal conductivity, and the rapid accumulation makes it as thermal blanketing that will cause slow heat dissipation. This insulating effect is also proposed to account for relatively high gradient in the shallow formation.

3 THERMAL CONDUCTIVITY

On the basis of nearly 200 previous published data of thermal conductivity in Tarim basin, 747 samples from 35 boreholes are measured in this study as supplementation to construct the complete dataset of thermal conductivity in this basin. The lithological type of samples is diverse, including the terrigenous sedimentary rocks as the mudstone, sandstone and conglomerate, the endogenous sedimentary rocks as limestone, dolomite, salt and coal rock, and igneous rocks as basalt, volcanic breccia, tuff, tuff lava and dacite and granitic diorite, and metamorphic rocks of phyllite and gneiss as well. These rocks are totally representative of types encountered in the sedimentary cover and crystalline basement of the Tarim basin. The geological age of formations from which these samples are taken is from Precambrian to Neocene. The sites of boreholes from which the core samples are retrieved nearly cover all the tectonic units of this basin, such as the northeast depression, Central uplift and the Maigaiti slope area and Yecheng sag of the Taxinan depression. Consequently, the measured data of thermal conductivity in this paper is the most representative for geothermal study.

The optical scanning method is used here to measure the thermal conductivity of all the samples, and this apparatus was manufactured by the German TCS company with an accuracy of ±3% for measurement ranging from 0.2 to 25 W/(m·K). However, the thermal conductivity of samples is determined in the core archive room under dry condition and air temperature. In order to retrieve the in-situ data of thermal conductivity, the corrections of water saturation, temperature and pressure effects are all required. Considering the prominent dominance of sedimentary rocks with various porosities in these samples, water saturation correction is indispensable. In this study, the geometrical mean model is adopted as water saturation correction for the sandstone and mudstone samples taken from the burial depth above 5000 meters[10,11]. Additionally, previous studies have shown that the water saturation correction for the limestone and dolomite are neglectable, due to their lower porosity and sufficient consolidation associated with large enough burial depth[5], so we make no correction for the carbonate rocks of limestone and dolomite. Accordingly, the thermal conductivity database of rocks in the Tarim basin of different geological time and lithological types are all constructed, on the basis of previous and measured values in this study, as shown in Table 2.

Table 2 Compilation of measured thermal conductivity data in Tarim basin

Age	Lithology	Thermal conductivity (W/(m·K))	Mean±SD (W/(m·K))	Numbers (N)
N	Mudstone	1.042∼2.559	1.778±0.372	31
	Sandstone	0.588∼3.020	1.68±0.618	55
	Limestone	1.507∼1.725	1.58±0.126	3
	Salt rock	4.245∼5.121	4.849±0.406	4
E	Mudstone	1.135∼3.023	1.883±0.447	17
	Sandstone	0.95∼3.926	1.961±0.522	41
	Conglomerate	1.125∼2.279	1.901±0.385	9
	Dolomite	3.078∼3.996	3.492±0.465	3
K	Mudstone	1.519∼2.424	1.908±0.264	18
	Sandstone	0.523∼2.958	1.565±0.662	45
	Conglomerate	1.336∼3.929	2.521±0.748	11
	Coal	0.246	0.246	1
J	Mudstone	2.1∼2.441	2.225±0.132	5
	Sandstone	1.299∼2.823	1.967±0.424	26
	Conglomerate	1.799	1.799	1
T	Mudstone	1.5∼3.374	1.934±0.481	14
	Sandstone	0.738∼3.241	1.547±0.59	50
	Conglomerate	0.786∼1.992	1.227±0.527	5
	Limestone	1.762∼3.213	2.596±0.75	3

Continue

Age	Lithology	Thermal conductivity (W/(m·K))	Mean±SD (W/(m·K))	Numbers (N)
P	Mudstone	1.321∼3.478	2.325±0.562	21
	Sandstone	0.952∼3.218	1.997±0.617	16
	Conglomerate	0.867∼1.763	1.205±0.388	4
	Dolomite	2.450∼2.632	2.541±0.129	2
	Basalt	0.94∼1.396	1.177±0.205	4
	Breecia	1.78	1.78	1
	Tuff	1.471∼2.221	1.846±0.53	2
	Tuff Lava	1.483∼1.705	1.594±0.157	2
	Limestone	1.875∼2.391	2.085±0.186	7
C	Mudstone	1.209∼3.312	2.216±0.435	51
	Sandstone	1.064∼4.436	2.441±0.619	46
	Conglomerate	1.81∼3.832	2.487±0.769	7
	Salt rocks	3.943∼4.382	4.163±0.31	2
	Dolomite	1.807∼4.387	2.932±0.77	9
	Coal	0.251	0.251	1
	Limestone	1.105∼3.652	2.211±0.481	54
D	Mudstone	2.535∼2.721	2.628±0.132	2
	Sandstone	1.480∼4.371	2.644±0.642	23
S	Mudstone	1.397∼3.544	2.203±0.375	32
	Sandstone	1.471∼4.482	2.646±0.685	68
	Conglomerate	1.503∼2.703	2.362±0.575	4
	Basalt	1.572	1.572	1
O	Mudstone	1.79∼4.023	2.673±0.67	18
	Sandstone	1.716∼4.911	2.676±1.128	8
	Conglomerate	2.202∼2.452	2.328±0.125	3
	Dolomite	2.322∼4.782	3.418±0.826	16
	Limestone	1.580∼5.315	2.578±0.696	115
∈	Mudstone	2.129∼4.277	3.446±0.801	10
	Dolomite	2.341∼5.224	3.718±0.676	45
	Limestone	1.825∼4.482	3.107±0.829	10
Z	Mudstone	2.512	2.512	1
	Sandstone	2.309∼3.533	2.921±0.866	2
	Dolomite	3.451	3.451	1
	Dacite	2.172∼2.257	2.215±0.06	2
	Granite	1.939∼2.319	2.125±0.19	3
AnZ	Phyllite	2.498∼2.722	2.610±0.158	2
	Quartz	2.444∼2.954	2.699±0.361	2
	Gneiss	2.053∼2.186	2.120±0.094	2

Measurement results show that the thermal conductivity of rocks of the Tarim basin varies from 0.246 W/(m·K) to 5.315 W/(m·K), but mainly concentrates in the range of 1.5∼2.5 W/(m·K) with a mean of 2.304 W/(m·K) (Fig. 5). The highest thermal conductivity is found in the salt rock, with a mean value of 4.620 W/(m·K). The lowest value of thermal conductivity is observed in the coal sample, ranging from 0.246 to 0.251 W/(m·K) with a mean of 0.249 W/(m·K). The thermal conductivity is dependent on mineral composition, porosity and fill of the porosity. Usually, the quartz content of the rocks is positively correlated with thermal conductivity, and the rocks in which clay content prevails show distinctively lower value than rocks with sand content. Variation of thermal conductivity of rocks in the Tarim basin reflects difference in composition, porosity

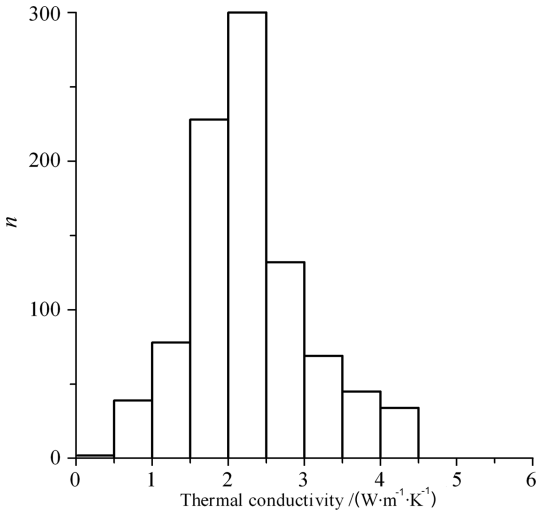

Fig. 5 Histogram of thermal conductivity in Tarim basin

and filled materials; and detailed discussion of thermal conductivity is beyond the scope of this paper.

We should mention that, due to sampling limits, the thermal conductivity of rocks retrieved directly from the intervals of borehole in which heat flow is determined is not available. When calculating the heat flow of the concerned interval in a borehole, the mean thermal conductivities of different lithological types in each formation are obtained firstly, and the thermal conductivity of each formation is then determined based on weighted average of the thermal conductivity of lithological types constituting the formation, according to lithological proportion in formation. Then the thermal conductivity of the interval is calculated using harmonic average of formation thickness.

4 HEAT FLOW

According to the geothermal gradient and thermal conductivity obtained in former section, 27 new heat flow values are determined in this study. To make good coverage in each main tectonic areas of the Tarim basin, 11 heat flow values are also estimated based on gradient derived from formation testing temperature data. These new retrieved values and related information are listed in Table 3. 25 previous published heat flow values in this area[4,5,8] are combined with our new results to give an updated map of present-day heat flow distribution in Tarim basin (Fig. 6).

The heat flow value in Tarim basin ranges from 26.2 to 65.4 mW/m^2, with a mean of 43.0±8.5 mW/m^2. As shown in Fig. 6, high heat flow is usually found in the uplift areas where the depth of the basement is relatively shallow, and is basically larger than 40 mW/m^2. For example, the average heat flow of the Katake uplift in the central Tarim basin is 55.4 mW/m^2, and 47.8 mW/m^2 for the Bachu uplift, 45.1 mW/m^2 for the Maigaiti slope area in the southwest Tarim baisn; the Guchengxu uplift has a heat flow of 54.6 mW/m^2, and the heat flow of the Shaya uplift area in the north Tarim is 40.9 mW/m^2. While for the depression areas with large basement depth, the heat flow is usually lower than 40 mW/m^2. For instance, the average heat flow of the Tanggubasi depression in the south Tarim basin is low as 39.6 mW/m^2, and that of the Yecheng depression in the south-

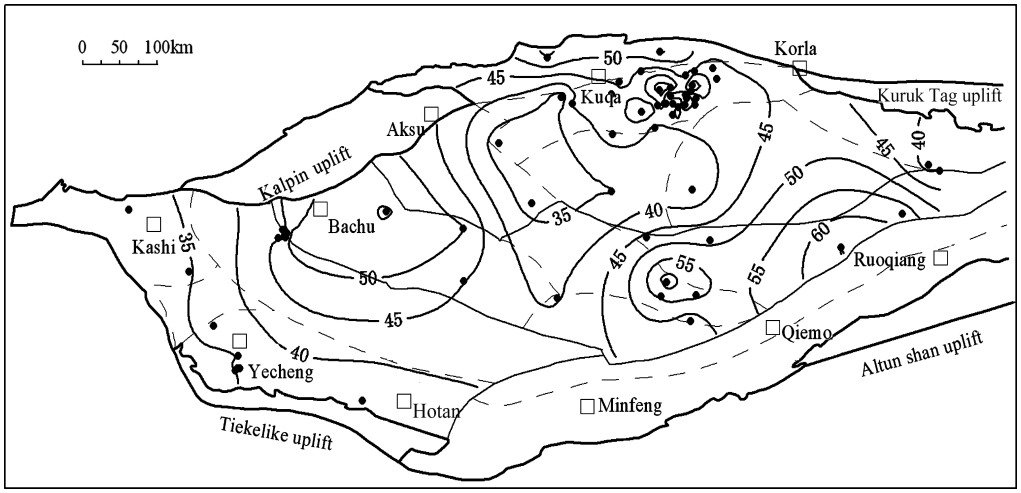

Fig. 6 Distribution pattern of present-day heat flow in Tarim basin

west is 35.6 mW/m^2. The lowest heat flow is observed in the Kashi and Awat depressions in the west Tarim basin as 33 mW/m^2 and 32.6 mW/m^2, respectively. However, the Kuqa depression in the north is characterized by high heat flow with a value of 51 mW/m^2, in contrast with low heat flow observed in other depressions of this basin. Local tectonic deformation induced heat contribution is proposed for this anomalous heat flow and will be discussed in later section. Consequently, lateral variation of heat flow in the basin is mainly influenced by the configuration and depth of the basement, along with local tectonic effect as well.

Table 3 New determined heat flow data in Tarim basin

No.	Well	Longitude	Latitude	Depth range	Gradient(°C/km)		Thermal Cond.	Q_0
		(E)	(N)	(m)	Mean±SD	Coefficient	(W/(m·K))	(mW/m^2)
1	Batan 2	78°03′16″	39°26′21″	1002550	23.5±0.57	0.999	1.841	43.3
2	Batan 3	78°02′50″	39°26′38″	100∼2350	21.8±1.17	0.997	1.981	43.2
3	Maican 1	78°00′49″	39°24′07″	500∼4155	20.0±0.89	0.999	2.028	40.6
4	Mai 2	78°01′50″	39°23′23″	250∼4000	22.0±1.46	0.999	2.260	49.7
5	HYC 1	88°05′56″	40°18′06″	100∼3820	20.5±1.70	0.998	1.841	37.7
6	Shenghe 1	79°18′01″	37°06′20″	4300∼5200	16.2±0.85	0.987	2.179	35.3
7	Dagu 1	83°35′31″	41°45′27″	75∼6291	19.7±1.39	0.999	2.234	44.0
8	Xinghuo 1	82°19′15″	41°26′44″	5000∼6147	14.8±0.39	0.998	2.14	31.7
9	Tangbei 2	82°14′45″	38°35′51″	300∼4900	19.8±1.17	0.999	2.000	39.6
10	Yingke 1	76°32′57″	38°53′13″	150∼4000	17.9±0.57	0.999	1.927	34.5
11	Yuqi 1	84°26′05″	41°33′34″	100∼5000	18.3±0.87	0.999	1.429	26.2
12	Yuqi 3	83°52′09″	41°31′04″	3700∼6100	16.6±0.69	0.998	1.853	30.8
13	Yuqi 4	83°59′50″	41°31′56″	3700∼5770	19.1±0.49	0.999	1.768	33.8
14	Sha112-2	83°46′30″	41°00′05″	3650∼6500	17.5±0.57	0.999	2.182	38.2
15	Sha 110	84°06′43″	41°09′50″	3800∼5600	19.3±0.51	0.999	2.238	43.2
16	Sha 71	83°49′01″	41°19′42″	4500∼5700	22.4±1.85	0.977	2.048	45.9
17	Sha 68	84°08′00″	41°18′05″	300∼2245	22.6±1.52	0.994	1.364	30.8
18	Sha 62	84°02′57″	41°21′22″	4500∼5750	25.0±0.95	0.996	2.114	52.9
19	Sha 55	83°31′02″	41°13′55″	5250∼5500	21.4±0.26	0.993	2.309	49.4
20	Sha 48	83°57′15″	41°20′05″	4150∼5280	15.8±1.80	0.953	1.944	30.7
21	Sha 47	83°59′44″	41°19′28″	4000∼5500	19.2±0.96	0.994	1.949	37.4
22	Sha 46	84°27′17″	41°16′36″	4000∼4500	19.5±0.14	0.999	1.779	34.7
23	DK 11	84°27′15″	41°17′26″	4200∼4500	24.6±0.63	0.977	1.776	43.7
24	Xinghuo 2	82°29′21″	41°20′50″	5350∼5630	15.5±0.37	0.978	2.646	41.0
25	Zhong 4	84°22′47″	38°37′14″	1900∼6080	20.2±1.55	0.998	2.773	56.0
26	Tazhong 1	83°55′41.3″	38°48′39.4″	5000∼6370	16.6±0.36	0.999	3.798	63.0
27	Manxi 1	83°06′29.8″	40°06′00.2″	3720∼4072	21.1±0.33	0.994	1.650	34.8
28	Manxi 2*	81°51′11″	39°56′09″		19.4		1.686	32.7
29	Mancan 1*	84°21′33″	40°06′56″		20.7		1.700	35.2
30	Tadong 1*	87°37′42″	39°40′32″		25		2.341	58.5
31	Tadong 2*	86°38′48″	39°14′04″		28.3		2.310	65.4
32	Tazhong 33*	83°38′05″	39°26′51″		22		2.086	45.9
33	Tazhong 32*	84°37′06″	39°23′49″		24.4		1.996	48.7
34	Tazhong 25*	84°16′28″	38°15′24″		24.3		1.933	47.0
35	Tazhong 3*	83°50′10″	38°36′54″		26		2.136	55.5
36	Fang 1*	79°35′12″	39°47′23″		18.2		3.048	55.5
37	He 4*	80°47′07″	39°34′07″		19.7		2.562	50.5
38	Shengli 1*	81°20′30″	40°46′39″		22.5		1.430	32.2

Note: mark * means estimated heat flow value.

5 DISCUSSION

5.1 Thermal Regime of Tarim Basin

Our results show that the present-day geothermal gradient of the Tarim basin ranges from 17 °C/km to 32 °C/km, with a mean of 22.6±3.0 °C/km. Compared with gradients of other large and middle scale basins in China listed in Table 4, this geothermal gradient of the Tarim basin is relatively low, suggesting it as cold basin with low temperature, coincident with previous understanding of this basin. Furthermore, the Tarim basin shares the similar geothermal regime with other typical craton basins in the world, such as the Michigan basin (22 °C/km)[23], Williston basin (<25 °C/km)[22] and Paraná basin of Brazil (22 °C/km)[25], so the Tarim basin is considered as one craton basin in thermal regime.

Table 4 Contrasting geothermal regime between different basins in China and cratons in the world

East China		Central China		West China		Craton basins in the world	
Basin	G, Q_0	Basin	G, Q_0	Basin	G, Q_0	Basin	G, Q_0
Jiyang[12,13]	36,66	Ordos[17]	29,62	Tarim	22.6,43	Williston[22]	<25,49
Hailaer[14]	30,55	Qinshui[18]	28,63	Qaidam[21]	288,53	Michigan[23]	22,42∼54
Subei[15]	30,68	Sichuan[19]	21,54	Junggar[21]	23,42.3	Ilinois[24]	19,48
Songliao[16]	37,69	Chuxiong[20]	28,76	Tuha[16]	25,44.5	Paraná[25]	22,56

Note: G is the geothermal gradient (°C/km) and Q_0 is surface heat flow (mW/m^2).

The heat flow of the Tarim basin varies from 26.2 mW/m^2 to 65.4 mW/m^2, with a mean value of 43±8.5 mW/m^2. This value is very similar to the heat flow values of some Precambrian shields, such as the India Shield of 25∼50 mW/m^2[26] and Canadian Shield of 42 mW/m^2[27], and craton basins as Michigan basin (42∼54 mW/m^2)[23], Williston basin (49 mW/m^2)[22] and Paraná basin of Brazil (56 mW/m^2)[25]. Accordingly, thermal regime study presented here indicates that the Tarim basin belongs to tectonically stable craton block and its heat flow is also relatively low compared with other basins in China. Generally, the geothermal regime of the Tarim basin is characterized by low heat flow and temperature, similar to those of typical craton basins in the world.

5.2 Factors that Influence Geothermal Regime of Tarim Basin

Tectonic setting of the basin is one first-order factor that controls present-day geothermal characteristics. Geophysical observations have shown that the Tarim basin is featured by large lithospheric thickness and strength, low temperature at Moho discontinuity, along with flexure deformation as a whole associated with the India-Asia collision[28], indicating the very weak activity of lithospheric dynamics, without more heat contribution from mantle. Furthermore, as a craton with the Precambrian continental crust, the Tarim basin is also tectonically stable, and no obvious magmatism and deformation occurred during Meso-Cenozoic. So the combination of weak lithospheric dynamics and quiet tectonic deformation may explain the low geothermal regime of the Tarim basin.

However, the distribution pattern of present-day geothermal field of the basin is also influenced by the basement configuration and contrasting thermal physical properties of rocks as well. As discussed in former section, it is found that high heat flow and geothermal gradient occur in the uplift areas, while low geothermal regime is observed in the depression areas. This pattern of geothermal field is a result of basement configuration within basin. Usually, the sediments accumulated in the depression area are composed of mudstone and sandstone basically, and the thermal conductivity of sediments is relatively low, compared with that of rocks in adjacent uplift area. This laterally contrasting thermal conductivity between the uplift and depression results in heat redistribution and the heat flows naturally from the depression to uplift where the thermal resistance is the smallest. This observed lateral variation of heat flow in the basin is termed as thermal refraction effect[29,30], and other factors, such as the depth of basement, difference in physical properties of diverse rocks

concerned, determine the effect extent of basement configuration on heat flow distribution, and will need further investigation.

However, some anomalous phenomena, contrary to the general pattern mentioned above, are also found in the Tarim basin, reflecting the influence of local structure on geothermal field. For example, the geothermal gradient in the northern Bachu uplift is relatively low, although it is located in the uplift area where the gradient is supposed to be high. Regional geological surveys have shown that the basement depth of this area is really shallow, even exposed to surface, which makes heat dissipate rapidly, considering large thermal conductivity of rocks. This is the reason for the observed low gradient heat flow in this area. Especially, the heat flow and gradient of the Kuqa depression are relatively large, with the values of 51 mW/m^2 and 26∼28 °C/km, respectively, even larger than those of the surrounding uplift areas. Two reasons are suggested here to explain this anomaly: firstly, located at the joint area of the Tianshan and Tarim basin, the Kuqa depression accommodates much sediment eroded directly from the Tianshan, and the thickness is even up to 11 km; this sediment is abundant in radiogenic element and contributes much radiogenic heat to surface heat flow. On the other side, seismic profilings have indicated that the Tarim block is now underthrusting below the Tianshan, the frictional heating derived from this subduction process and associated exhumation can disturb geothermal field in this area, which accounts for the observed high temperature and heat flow in the Kuqa depression.

5.3 Relationship Between Oil/Gas Field and Geothermal Gradient

Comparing the distribution of discovered oil and gas field with the geothermal gradient map in Tarim basin, it is found that all the discovered oil and gas fields are nearly coincident with areas of high geothermal gradient, and the gradient of gas field is usually larger than that of the oil field. For example, the Kelasu tectonic belt where the Kela No.2 large scale natural gas field is discovered, and the Qiulitage tectonic belt in which the Dina No.2 gas field is located, are all accompanied by geothermal gradient as high as 26∼28 °C/km. The gradient of the Hetianhe (Hotan River) gas field in the south of the Bachu uplift is also relatively high, and is 2∼6 °C/km larger than that of surrounding area. Interestingly, previous studies have shown that the gradient of Shacan No.2 well, a very high productive oil well of the Yakela area in the north Tarim basin, is also larger than those of adjacent regions[6]. On the basis of investigating case studies in literatures, it is found that similar situations exist in numerous fields in other parts of the world. Fei and Liu[31] indicated that most oil and gas fields in the Dongtai depression of the Subei basin in East China are accompanied by high geothermal gradient as 35∼40 °C/km, and the discovered oil and gas fields in the Liaodong bay of north China are mostly located in the Liaoxi uplift area where the gradient is large[32]. This observation is also found in the Yinggehai basin in the northern margin of the South China Sea, where the discovered gas fields are characterized by really high geothermal gradient[33]. On the basis of superposing the maps of geothermal gradient with discovered gas field map in China, Zhou et al.[34] proposed that all the gas fields are discovered in areas with high geothermal gradient, regardless of the thermal regime of whole basin being hot or cold. Previous studies have shown that most oil and gas fields in the Rocky Mountain areas and mid-United States and some oil fields in former Soviet Union such as the Wild gorge, Bakhar and Voyvozhsky fields are all accompanied by positive temperature anomaly[35∼37], and these data also suggested that the temperature anomaly magnitude in gas field is larger than that in the oil field.

Although the fact that oil and gas fields are accompanied by high geothermal gradient or positive temperature anomaly is well recognized in the world, the mechanism and cause for this coincidence are still ambiguous. The proposed hypothesis includes heat redistribution associated with lateral difference in thermal physical properties of rocks, heterogeneities of base heat flow, thermal effects of magma intrusion and tectono-thermal event, shallow radiogenic heating and contributions from some physical-chemical process that can produce heat, and upward movement of thermal fluid below[35∼37]. As one tectonically stable basin, the Tarim basin has not experienced obvious tectonic-thermal events and associated magmatism since Late Paleozoic, and the heat distribution derived from difference in properties of rocks and radiogenic heat contribution from sediments are all introduced to account for the observed geothermal pattern that high geothermal gradient exists in the uplift and

low in other depression areas except for the Kuqa depression where the gradient is strangely high in the Tarim basin, as discussed in former section. However, the discovered oil and gas fields are not limited only to those uplift areas and the Kuqa depression that are of high geothermal gradient, for example, the gradient in the south of the Bachu area is relatively low as 22 °C/km, but the discovered Hetianhe gas field is with high gradient as 24∼26 °C/km in this low area. Other mechanism is needed to explain this positive geothermal gradient anomaly occurred in oil and gas field. It is common that fluid can migrate along fault conduit and accumulate at the structural trap, along with the movement of hydrocarbon and heat, driven by tectonic contraction from basin boundary and thermal-mechanical process within basin, so the upward and lateral movement of subsurface heat fluid along fault is speculated as the major cause for this observed geothermal anomalies.

It is long recognized that the generation of oil and gas is determined by the paleo-geothermal evolution of hydrocarbon rocks during its geological history, so the studies of paleo-geothermal field of sedimentary basin are essential in petroleum geology. However, our results presented here indicate that present-day geothermal regime can offer clue to seek for potential oil and gas field, suggesting its possible role in oil and gas exploration. We call for efforts of conducting high resolution continuous temperature logging and measurement of thermal physical properties such as heat production, thermal conductivity and density and etc, to decipher the present-day geothermal gradient and subsurface temperature within basin accurately. On the basis of the structural and stratigraphic traps, the geothermal trap constrained by present-day geothermal regime is integrated to improve efficiency of finding oil and gas field.

6 CONCLUSIONS

Compared with other basins in China, the present-day geothermal gradient and heat flow of the Tarim basin are really low, with a mean of 22.6±3.0 °C/km and 43.0±8.5 mW/m^2, respectively. Considering its low geothermal regime, the Tarim basin is undoubtedly regarded as one typical craton basin in the world.

Heat flow and geothermal gradient is relatively high in the uplift areas where the depth of basement is shallow, and is low in the depression areas, indicating the first order control of basement configuration on geothermal characteristics. However, this pattern is also affected by local structures, and the Kuqa depression is a good example, where the heat flow and gradient is relatively high, resulted from the combined effects of crustal radiogenic contribution and tectonic heating from Cenozoic deformation between the Tianshan Mountain and Tarim basin. Other factors, such as deep structure, tectonic evolution of basin and hydrocarbon accumulation, also can affect the geothermal regime of the basin.

The discovered oil and gas fields in the Tarim basin are generally accompanied by high geothermal gradient or positive temperature anomaly, and the upward and lateral movement of subsurface heat fluid along fault as conduit is considered as the major cause for this anomaly and need further investigation. Results presented here indicate that the accurate geothermal study is of significance for oil and gas exploration as supplementary tool.

ACKNOWLEDGMENTS

This research is financially supported by National Nature Science Foundation of China (40504013), CNPC Innovation Fund (07E1033) and Sinopec Marine Strategic project. We thank the Northwest Oilfield Branch of Sinopec for assistance during in-situ thermal conductivity measurement, and Dr. Meijun Li of China University of Petroleum-Beijing is thanked for help in temperature data collection. Dr. Shengbiao Hu of Institute of Geology and Geophysics, CAS, is appreciated for providing the optical scanning apparatus used in this study and useful discussion. We also thank anonymous reviewers for constructive suggestions.

REFERENCES

[1] Jia C Z ed. Structural Characteristics and Hydrocarbon in Tarim Basin of China (in Chinese). Beijing: Petroleum

Industry Press, 1997. 1∼274

[2] Wei D W. Terrestrial heat flow on the northern side of Tarim basin. *Chinese Journal of Geology* (in Chinese), 1992, **27**(1): 93∼96

[3] Zhang H R, Liu G B. The hydrocarbon occurrence and characteristics of geothermal field in Tarim basin. *Xinjiang Petroleum Geology* (in Chinese), 1992, **13**(4): 294∼304

[4] Wang L S, Li C, Shi Y S. Distribution of terrestrial heat flow density in Tarim basin, western China. *Chinese J. Geophys.* (in Chinese), 1995, **38**(6): 855∼856

[5] Wang J, Wang J A, Shen J Y, et al. Heat flow in Tarim basin. *Earth Science-Journal of China University of Geosciences* (in Chinese), 1995, **20**(4): 399∼404

[6] Xie D Y. Geothermal characteristics in northern Tarim basin, northwestern China. *Earth Science-Journal of China University of Geosciences* (in Chinese), 1993, **18**(5): 627∼634

[7] Wang L S, Li C, Liu S W, et al. Geothermal gradient distribution of Kuqa foreland basin, north of Tarim, China. *Chinese J. Geophys.* (in Chinese), 2003, **46**(3): 403∼407

[8] Wang L S, Li C, Liu S W, et al. Terrestrial heat flow distribution in Kuqa foreland basin, Tarim, NW China. *Petroleum Exploration and Development* (in Chinese), 2005, **32**(4): 79∼83

[9] Qiu N S. Characters of thermal conductivity and radiogenic heat production rate in basins of northwest China. *Chinese Journal of Geology* (in Chinese), 2002, **37**(2): 196∼206

[10] Woodside W, Messmer J. Thermal conductivity of porous media: I. Unconsolidated sands. *Journal of Applied Physics*, 1961, **32**: 1688∼1699

[11] Woodside W, Messmer J. Thermal conductivity of porous media: II. Consolidated sands. *Journal of Applied Physics*, 1961, **32**: 1699∼1706

[12] Gong Y L, Wang L S, Liu S W, et al. Distribution characteristics of geotemperature field in Jiyang depression, Shandong, north China. *Chinese J. Geophys.* (in Chinese), 2003, **46**(5): 652∼658

[13] Gong Y L, Wang L S, Liu S W, et al. Distribution characteristics of terrestrial heat flow density in Jiyang depression of Shengli Oilfield, East China. *Science in China* (*Series D*), 2004, **47**(9): 804∼812

[14] Cui J P, Ren Z L, Su Y, et al. Relationship between present geotemperature and hydrocarbon generation in Haila'er basin. *Petroleum Exploration and Development* (in Chinese), 2007, **34**(4): 445∼450

[15] Wang L S, Shi Y S. Geothermal Study on the Oil and Gas Basin (in Chinese). Nanjing: Nanjing University Press, 1989

[16] Ren Z L. Tectono-Thermal Evolution in Sedimentary Basins, North China (in Chinese). Beijing: Petroleum Industry Press, 1999

[17] Ren Z L, Zhang S, Gao S L, et al. Tectonic thermal history and its significance on the formation of oil and gas accumulation and mineral deposit in Ordos basin. *Science in China* (*Series D*), 2007, **50**(Suppl.II): 27∼38

[18] Sun Z X, Zhang W, Hu B Q, et al. Features of heat flow and the geothermal field of the Qinshui basin. *Chinese J. Geophys.* (in Chinese), 2006, **49**(1): 130∼134

[19] Yuan Y S, Ma Y S, Hu S B, et al. Present-day geothermal characteristics in south China. *Chinese J. Geophys.* (in Chinese), 2006, **49**(4): 1118∼1126

[20] Wang G L, Cai L G, Wang J Y, et al. Paleo-geothermal field and tectonic-thermal evolution in the Chuxiong basin of China. *Petroleum Geology and Experiment* (in Chinese), 2005, **27**(1): 28∼38

[21] Qiu N S, Hu S B, He L J. Principles and Progresses on Thermal Regime of Sedimentary Basins (in Chinese). Beijing: Petroleum Industry Press, 2004

[22] Osadetz K G, Kohn B P, Feinstein S, et al. Thermal history of Canadian Williston basin from apatite fission-track thermochronology-implications for petroleum systems and geodynamic history. *Tectonophysics*, 2002, **349**: 221∼249

[23] Speece M A, Bowen T, Folcik J L, et al. Analysis of temperature in sedimentary basins: the Michigan basin. *Geophysics*, 1985, **50**(8): 1318∼1334

[24] Davis H G. Pre-Mississippian hydrocarbon potential of the Illinois basin. In: Leighton M W, Kolata D R, Oltz D F eds. Interior Cratonic Basins. *American Association of Petroleum Geologists Memoir*, 1990, **51**: 473∼489

[25] Hurter S J, Pollack H N. Terrestrial heat flow in the Paraná Basin, southern Brazil. *Journal of Geophysical Research*, 1996, **101**(B4): 8659∼8671

[26] Roy S, Rao R U M. Heat flow in the Indian shield. *Journal of Geophysical Research*, 2000, **105**(B11): 25587∼25604

[27] Jaupart J. Heat flow and thickness of the lithosphere in the Canadian Shield. *Journal of Geophysical Research*, 1998, **103**(B7): 15269∼15286

[28] Wang L S, Li C, Yang C. The lithospheric thermal structure beneath Tarim basin, western China. *Chinese J. Geophys.* (in Chinese), 1996, **39**(6): 794∼803

[29] Xiong L P, Gao W A. Characteristics of geotherm in uplift and depression. *Chinese J. Geophys.* (in Chinese), 1982, **25**(5): 448∼456

[30] Lin G C, Nunn J A, Deming D. Thermal buffering of sedimentary basins by basement rocks: implications arising from numerical simulations. *Petroleum Geoscience*, 2000, **6**: 299∼307

[31] Fei F A, Liu P H. The relationship between petroleum and geotherm in the Dongtai depression, northern Jiangsu. *Oil and Gas Geology* (in Chinese), 1981, **2**(1): 18∼27

[32] Li W L, Liu Z, Yu S, et al. Characteristics of geotemperature-geopressure fields and their relationships with distribution of oil and gas: taking Liaodong bay as an example. *Natural Gas Industry* (in Chinese), 2006, **26**(9): 17∼20

[33] Wang J Y, Xu J H, He L J, et al. Thermal history, tectonic-thermal evolution and activity of heat fluid of basins. In: Gong Z S ed. Dynamic Research of Oil and Gas Accumulation in Northern Marginal Basins of South China Sea (in Chinese). Beijing: Science Press, 2004. 65∼95

[34] Zhou Q H, Feng Z H, Men G T. Present geothermal regime and its relationship to natural gas generation in Xujiaweizi faulted depression, north Songliao basin. *Science in China* (*Series D*) (in Chinese), 2007, **37** (Suppl.II): 177∼188

[35] Meyer H J, McGee H W. Oil and gas fields accompanied by geothermal anomalies in Rocky Mountain Region. *AAPG*, 1985, **69**(6): 933∼945

[36] McGee H W, Meyer H J, Pringle T R. Shallow geothermal anomalies overlying deeper oil and gas deposits in Rocky Mountain Region. *AAPG*, 1989, **73**(5): 576∼597

[37] Merriam D F. Subsurface temperature as a passkey for exploration of mature basins: hot anticlines-a key to discovery? *Oil and Gas Journal*, 2004, **102**(32): 29∼36